



\*DE01922328X\*



FR0301221

INIS-FR-1609

## Suppressing Hydrogen Ingress during Aqueous Corrosion of CANDU Zr-2.5 Nb Pressure Tube Material

M. B. ELMOSELHI<sup>1</sup>, A. DONNER<sup>1</sup>, A. BRENNENSTUHL<sup>1</sup>, B.D. WARR<sup>1</sup>  
D. W. EVANS<sup>2</sup>, P. J. ELLIS<sup>2</sup>,

### ABSTRACT

As a result of their special properties, including low neutron cross-section and intrinsic corrosion resistance, Zr alloys are used in the fabrication of nuclear core components, particularly fuel cladding (in most reactor types) and also Zr-2.5 Nb pressure tubes in CANDU<sup>®</sup> (Canada Deuterium Uranium) reactors. Corrosion and H uptake during service can limit the life of these components. Therefore, remedial action may be appropriate to slow the H uptake rate and prolong the working life of these reactor components.

This work has explored the possibility of reducing H uptake in pressure tube material by incorporating an inhibiting agent into the corrosion environment. Two approaches have been tested, depositing a thin metallic film on the initial oxide surface and adding an inhibiting agent to the solution. The latter approach appears more practical. Screening experiments were conducted in short-term (~30 day) exposures in high temperature (340°C) aqueous out-reactor environments, simulating the CANDU<sup>®</sup> heat transport coolant with various chemistries. Compounds tested included aluminum acetate, aluminum nitrate, lithium nitrate, rhodium nitrate and yttrium nitrate. Comparison of results from the aluminum nitrate additives and aluminum acetate additives suggests that the nitrate anion is the effective ingredient for H ingress inhibition. The nitrate anion appears to reduce the rate of H ingress regardless of the associated cation. However, each cation appears to affect the rate of corrosion differently. These cations were found to be incorporated in the oxide film.

---

<sup>1</sup> Kinectrics Inc.

<sup>2</sup> Ontario Power Generation Inc.

© CANDU is a registered trademark of Atomic Energy of Canada Ltd.

## 1. INTRODUCTION

Zirconium alloys are used in the fabrication of nuclear core components particularly fuel cladding (in most reactor types) and also as the Zr-2.5 wt.% Nb alloy in pressure tubes in CANDU<sup>®</sup> (Canada Deuterium Uranium) reactors. This is due to their special properties, including low neutron cross-section and intrinsic corrosion resistance. Since these alloys pick up hydrogen (H) in reactor heat transport coolants, hydride formation and delayed hydride cracking may occur, as well as changes in fracture toughness, at high H levels. Therefore, the build up of H in a reactor component could be life limiting. Inhibitors are being developed to reduce rates of H uptake and extend the working life of these components. The focus of this work is to identify an effective inhibitor which would be introduced into the reactor coolant, resulting in a reduction of H ingress in these components and particularly in CANDU<sup>®</sup> pressure tubes.

Very little work has been done in this area. Cox [1] had surveyed the subject briefly and reported that potential Zr hydrating inhibitors which have a significant effect on H pickup are sodium nitrite and oxygen. In other unpublished work, several elements were tested as inhibitors including compounds of the following elements: V, Cr, Fe, Ni, Cu, Zn, As, Mo, Sb and B [2]. The testing procedure consisted of autoclaving Zr-2.5Nb and Zircaloy-2 samples in aqueous solutions of compounds of these elements in 1.0M LiOH for 1 day at 340°C. Although the exposures were short-term, some elements showed promise in terms of reducing the corrosion rate. However, the effect on H ingress was undetectable, partly due to inadequate H analysis techniques being available at that time. Other chemical additions, for example boric acid have been shown to be effective corrosion inhibitors of crystal bar Zr and Zircaloy-2 in 500°C steam [3].

To explore the possibility of suppressing corrosion/ H ingress and to identify suppressants (inhibitors), we begin by briefly examining the current understanding of the salient mechanisms and reactions leading to the corrosion of Zr alloys, especially those aspects relevant to H ingress. The interaction of water molecules (H<sub>2</sub>O or D<sub>2</sub>O) with Zr surfaces results in the formation of an oxide and the liberation of H or D (deuterium) gas according to the following overall equation:

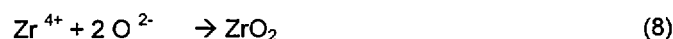
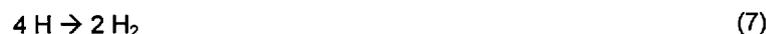
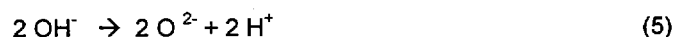


The majority of the generated H<sub>2</sub> (following recombination) dissolves in the corroding solution as H<sub>2</sub> gas, except for a small percentage that is absorbed by the bulk alloy as atomic hydrogen, constituting what is known as the % H uptake, where,

$$\% \text{ H uptake} = (\text{H entering alloy} / \text{H from corrosion}) \times 100 \quad (2)$$

The steady state % H uptake ranges from ~5 to 40% depending on the alloy. For example, for Zr-2.5Nb it is generally found to be in the range between ~5-10%.

Although, the mechanism of H evolution and ingress is not yet precisely understood, it is well established that it follows the overall equation (1) which may be the sum of the following reactions:



The first reaction (3) is the dissolution of Zr which represents the anodic oxidation or de-electronation reaction. It is well established that this reaction occurs at the metal-oxide interface, since the oxide in these alloys is known to proceed by inward growth with negligible migration of Zr cations to the oxide surface. Equations (4) and (5) show the dissociation of water molecules to produce H<sup>+</sup> and OH<sup>-</sup>. The cathodic reaction, equation (6), is represented here by the reduction or electronation of H<sup>+</sup> to produce H atoms followed by recombination (to produce H<sub>2</sub> gas) and

desorption into the solution (equation 7). Clearly this step in the overall reaction is critical in terms of H uptake by the bulk alloy. The locations where this reaction takes place within the alloy-oxide-solution system are still uncertain and may be critical in terms of controlling the uptake. It has been suggested that although most of the cathodic reaction may occur at the oxide-solution interface, electronation of protons may also take place at the alloy-oxide interface [4].

The cathodic electronation of protons results in adsorbed H atoms followed by recombination and desorption of H molecules into the solution. However, as mentioned, some H atoms may migrate across the oxide-metal interface and become absorbed by the bulk alloy. It has been reported that oxidized Nb absorbed tritium from the gas phase at room temperature in contrast to similar experiments with H or D [5]. This effect was ascribed to the dissociation of physisorbed tritium molecules by decay-produced electrons and X-rays. If dissociation of H molecules appears to accelerate the uptake by the bulk alloy, recombination and desorption are likely to result in a reduction in H ingress.

Therefore, an agent which increases the recombination and desorption (H evolution) reaction may result in a reduction of H uptake by the bulk alloy. Following this rationale, elements may be ranked in terms of their ability to catalyze the H evolution reaction according to the magnitude of their equilibrium exchange-current density for the reaction. From this point of view, elements as electrodes in  $\sim 1\text{M H}_2\text{SO}_4$ , are ranked in decreasing order of their ability to catalyze H evolution as follows: Pd, Pt, Rh, Ir, Ni, Au, W, Ti, Cd, Mn, Tl, Pb and Hg [5]. Work on the catalyzed recombination of H atoms by chemical means resulted in the establishment of the following decreasing order of catalytic activity: Pt, Pd, W, Fe, Cr, Ag, Cu, Pb and Hg [7]. This closely follows the results in reference [6], which may be an indication of a parallelism between catalysis and electrocatalysis.

Another possible inhibiting mechanism includes the co-adsorption of the inhibiting species along with H on the solid surface. For example, the adsorption of H on Pt [110] is totally inhibited when the surface is saturated by sulphur with a coverage of at least 0.8 (80% of a monolayer). The presence of sulphur was found to weaken the Pt-H bond [8]. Furthermore, metals such as Al, Au, Li, Na, K, Mg, Ag, Zn, Cd, In, Si, Ge, Sn, Pb, As, Sb and Bi, that do not appear to dissociate H, and may act as catalysts for recombination, could be potential ingress inhibitors [9].

Oxidation resistance and H uptake for Zr have been altered substantially by alloying it with other metals including Nb, Fe and Pd. The latter element (Pd) results in improved oxidation resistance when present as a thin layer in the case of Zircaloy-4 [10]. A deleterious effect of surface carbides has been found as a result of facilitating the transfer of electrons, thus promoting rapid oxidation [11]. Finally, the effect of various impurity elements in Zr-2.5Nb on corrosion and D pickup have been reported [12]. A favorable effect of Fe (in the range of 400-1300 mg/kg) has been deduced from results of long term out-reactor aqueous corrosion tests.

In view of all the above-mentioned possibilities, procedures for introducing the potentially inhibiting element into the corrosion environment, as well as (accelerated) testing procedures to examine their effects on corrosion and H ingress have been identified. Also, analytical methods to monitor the changes in oxide thickness, oxide microchemistry and H content of the samples were identified. The developed testing procedures and results from a limited number of elements tested are described in the following sections.

## 2. EXPERIMENTAL

In the first set of experiments, Zr-2.5 Nb coupons (10 x 20 x 1 mm) were machined from pressure tube material, autoclaved (400°C steam for 24 hours) and covered with thin ( $\sim 20$  nm) metallic films of Al & Pd. Impurity concentrations in the pressure tube material are shown in Table 1. The deposition was performed with a net mask to create squares of the film on the oxide so that portions of the oxide surface interact directly with the solution. Two sets of coated specimens and one uncoated (as a control set) were corroded in an autoclave with oxygenated ( $\sim 100$  mg/kg) de-ionized  $\text{H}_2\text{O}$  at 350°C for 7 days.

In the second set of experiments, Zr-2.5 Nb coupons (8 x 8 x 0.5 mm) were machined from the same pressure tube material and in this case the inside (ID) surfaces were preserved. One set of (three) coupons were in the as-received (bare) condition; these are expected to be very reactive and sensitive to different solution chemistries. The second set of (three) coupons was pre-filmed as above to produce an oxide film 0.5 to 1.5  $\mu\text{m}$  thick. Coupons were exposed in Inconel-600 static autoclaves and each solution was prepared by adding the selected compound of the element (cation) under consideration to  $\text{H}_2\text{O}$  to maintain a calculated 100 mg/kg concentration of the cation,

assuming that the compound is totally soluble. The room temperature pH was adjusted to ~ 9.84 (equivalent to an apparent pH (pH<sub>a</sub>) in the heavy water coolant of ~10.3) using LiOH. The solutions were purged with Ar+5% H<sub>2</sub> to remove O<sub>2</sub>, while controlling the dissolved H<sub>2</sub> to within 1-2 mg/kg at 340°C. The exposures were conducted at 340°C for 30 days.

Differential Scanning Calorimetry (DSC) was selected for H analysis. DSC is a virtually non-destructive technique so that multiple measurements can be made for the same sample. It determines the temperature of hydride dissolution completion. This temperature corresponds to a concentration that is equal to the terminal solid solubility (TSS) at that temperature. The measured temperature is converted into concentration using an established Arrhenius relation (TSS vs 1/T) with an accuracy of ± 5%. Another significant advantage of this technique is that [H] is measured in the alloy since the technique is insensitive to the H or moisture in the oxide covering the sample. Fourier transform infrared (FTIR) spectrometry was used to measure oxide thickness by measuring the spacing between the interference peaks [13].

The changes in microchemistry of the oxide exposed to the inhibiting agent were examined by through-oxide-thickness depth profiling using a Cameca IMS-3f Secondary Ion Mass Spectrometer (SIMS). The technique uses a beam of energetic (~ 10 KeV) Cs<sup>+</sup> primary ions rastered over an area 250 μm x 250 μm to sputter several atomic layers of the sample surface. The secondary ions from a region 60 μm in diameter are extracted by electric fields and the energy and mass of these secondary ions analyzed using a mass spectrometer. The intensities of several ions, depending on the particular solution chemistry being tested, were measured through the oxide and into the base alloy.

**Table 1**  
**Ingot Chemical Analysis for Pressure Tube H365M**

Element	Concentration (mg/kg) (except Nb)
Nb	2.5 weight %
O	1100
Al	47
C	130
Fe	457
H	5
Mo	< 25
Cu	< 25
N	32
Sn	35
U	1.5

\* balance Zr

### 3. RESULTS

The change in oxide thickness and [H] following the corrosion of pre-filmed samples with a thin Al and a thin Pd film are summarized in Table 2. Table 2 indicates that although the presence of the Al film appears to increase the corrosion rate (oxide thickness) compared to the reference samples, it decreases the net H uptake. On the other hand, the Pd film results in a slightly lower increase in oxide thickness compared to the reference coupons, but gave a higher value of H uptake.

**Table 2 - Average Change in Oxide Thickness and [H] for Zr-2.5 Nb Samples**  
(autoclaved in oxygenated (~100 mg/kg) de-Ionized H<sub>2</sub>O At 350 °C for 7 days)

Type of sample	Change in [H] (mg/kg) ± 2σ	Change in oxide thickness (σm) ± 2σ	Calculated % uptake
As-received samples (reference)	2.1 ± 0.3	1.2 ± 0.2	2.2
Samples coated with Pd film	3.3 ± 0.7	1.0 ± 0.1	4.2
Samples coated with Al film	1.3 ± 0.3	1.5 ± 0.3	1.1

Changes in [H] and oxide thickness of bare and prefilmed coupons following exposure in autoclaves with the different inhibiting agents are summarized in Table 3. The Table shows average values and standard deviations (σ) for each set of three samples. H uptake by the bulk alloy is indicated by the measured change in [H] (σ[H]) of the samples, given that the samples are macroscopically identical. Also, the calculated % H uptake, based on measured σ[H] and calculated H production using equation (2), is shown.

The values from each experiment should be compared with the results shown in the first column of Table 3, which represent samples exposed to a reference solution with no added inhibiting agent. Results from Table 3 are depicted graphically in Figures 1 and 2. The change of [H] for bare and prefilmed samples is shown in Figure 1, and the change in oxide thickness for both sample types is shown in Figure 2.

Secondary ion intensities versus depth for the Al in bare and pre-filmed samples are compared to profiles in reference samples in Figures 3. In Figure 4, H profiles are compared for bare samples exposed to a solution with aluminum nitrate and a reference solution.

**Table 3 - Average Change in Oxide Thickness and [H] for Zr-2.5 Nb Samples**  
(autoclaved in solutions of different chemistries at 340 °C for 30 days)

Element (cation)	Reference	Al	Al	Li	Rh	Y
<b>Potential Inhibiting Agent</b>	None	Aluminum acetate	Aluminum nitrate	Lithium nitrate	Rhodium (III) nitrate	Yttrium (III) nitrate
<b>Bare Coupons</b>						
<b>Increase in Oxide (σσm)</b>	1.9	1.8	2.0	3.6	2.2	2.6
σ (σm)	0.00	0.03	0.02	0.10	0.05	0.02
<b>Increase in [H] (mg/kg)</b>	90	100.3	11.2	11.9	12.4	11.5
σσ (mg/kg)	1.85	3.62	0.39	0.45	1.08	0.98
<b>% H Uptake</b>	35.3	46.1	4.6	2.6	4.8	3.2
σ (% Uptake)	1.38	2.69	0.20	0.05	0.78	0.17
<b>Prefilmed Coupons</b>						
<b>Increase in Oxide (σσm)</b>	0.7	0.7	0.8	2.3	1.1	1.3
σ (σm)	0.00	0.04	0.06	0.21	0.03	0.05
<b>Increase in [H] (mg/kg)</b>	4.4	4.1	3.3	3.2	3.0	2.9
σσ (mg/kg)	0.12	0.20	0.13	0.35	0.15	0.06
<b>% H Uptake</b>	5.1	5.6	3.8	1.2	2.5	1.9
σ (% Uptake)	0.07	0.39	0.55	0.11	0.01	0.20

## 4 DISCUSSION

Results from samples with a thin film of Al deposited on the oxide indicate that the presence of such a film reduces the H pickup by ~38%, although the corrosion rate was found to increase somewhat, as indicated in Table 2. For thin films of Pd, however, this trend was reversed, with a 57% increase in H pickup associated with a small reduction in corrosion rate. The effect may be attributed to the H dissociating capability of Pd over Al as previously discussed in Section 1.

Based on the above results it might be expected that compounds containing Al would be effective inhibitors when added to aqueous environments. However, the results from exposures to aqueous environments containing aluminum acetate shown in Table 3 and Figure 1, indicate otherwise. For both bare and prefilmed samples, the change in [H] is practically the same with or without the addition of this compound. Therefore, although Al was found to be an effective inhibitor as a coating, it is ineffective when added as an acetate compound to a solution.

Aluminum nitrate was also tested, since, as discussed in Section 1, sodium nitrite was found to be an effective inhibitor of H ingress in Zr alloys [1]. Nitrates were presumed more soluble than nitrites. Results from the aluminum nitrate tests, particularly for bare samples, shown in Table 3 and Figure 1, show that it is indeed an effective inhibitor for H ingress with an ~88% reduction in H ingress compared to the reference. Also, the rate of corrosion is practically unchanged, as shown in Figure 2. Since the nitrate anion appears to be the critical inhibiting species with respect to H uptake, other nitrate-containing compounds were tested.

As shown in Figure 1, these other nitrate compounds, i.e. lithium, rhodium and yttrium nitrate, also showed similar H uptake inhibition with reductions of ~90% in H uptake in the case of the bare samples. For prefilmed samples, all nitrate-containing compounds showed an inhibiting effect, although the effect is less pronounced, with reductions of ~26%.

The beneficial effect of the nitrate anion on H uptake in these exposures may be related to its role in the production of ammonia from H liberated by the corrosion reaction, equation 1. Such a mechanism has been proposed for the beneficial effect of calcium nitrate on the highest yield of cubic zirconia obtained during hydrothermal oxidation of Zr in the presence of nitrate [14]. The generalized form of the equation we propose for aluminum nitrate is as follows:



where the Greek symbols represent coefficients which require experimental determination. As is evident from this equation, and comparison to the usual Zr/water reaction, equation (1), the formation of ammonia is associated with a significant reduction in the H available for pickup by the alloy. Also, the cation species, in this case Al, is incorporated in the growing oxide. In order to confirm the above hypothesis, a colorimetric analysis method was used to determine the concentration of the ammonium ion ( $\text{NH}_4^+$ ) in water. The reduction of nitrate to ammonia was confirmed by the detection of 6.90 and 5.65 mg/kg of ammonia in the post-exposure solutions containing aluminum nitrate and yttrium nitrate respectively. No ammonia was found in the post-exposure reference solution or the other non-nitrate solution containing aluminum acetate.

With reference to Table 3 and Figure 2, for both bare and prefilmed samples, in all cases higher (effective) corrosion rates were found in the case of nitrate additions than for the reference solution. Also, the type of cation appears to play a role on corrosion performance where corrosion rate increased from Al to Rh to Yt and finally the presence of Li resulted in the highest corrosion rate.

Through-oxide-thickness elemental concentration profiles obtained using SIMS show clear evidence of the incorporation of cations in the oxide. Depth profiles of  $^{90}\text{Zr}$  were obtained for selected samples in order to provide a reference against which the profiles for other species could be compared. Note that in SIMS, the relative intensities of a given element provide a qualitative indication of its relative concentration. The  $^{90}\text{Zr}$  intensity profile is also used to identify the oxide-metal interface, i.e. where the  $^{90}\text{Zr}$  intensity drops off. This may be slightly different from the measured value of oxide thickness using FTIR shown in Table 3, which can be attributed to the assumptions used to convert the sputtering time to depth.

The incorporation of Al into the oxides grown on a bare sample and a pre-filmed sample is illustrated in Figure 3a and 3b respectively. The Al depth profiles of the two reference samples are omitted in Figure 3a for clarity. In general, Al appears to be enhanced within the oxide and particularly near the oxide surface and especially in the case of the bare sample. Also, it is noted that the outer surface of the oxide accommodates more Al than the bulk

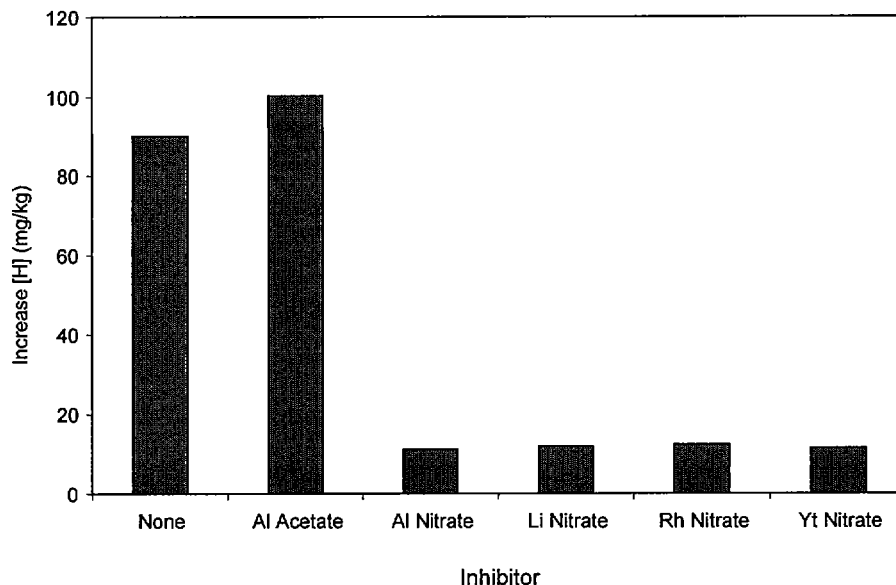
oxide, possibly through an ion exchange sorption process. The incorporation of Al is almost two orders of magnitude higher following exposures to solutions containing aluminum acetate, as shown in Figure 3. Therefore, the chemistry of the compound seems to have a significant influence on the extent of the incorporation into the oxide. No obvious correlation was found between the extent of the cation incorporation and the corrosion rate.

The significant reduction in H uptake observed for the bare samples when corroded with nitrate additives may be confirmed by through-thickness depth profiling of H. Figure 4 shows H depth profiles for two macroscopically identical bare samples; one was autoclaved in a reference solution while the second was autoclaved with the aluminum nitrate additive. It is clear that qualitatively the sample exposed in the reference solution contains a significantly higher [H] in the bulk alloy than that exposed to aluminum nitrate. This is consistent with the analytical results. The sample exposed to aluminum nitrate, however, appears to contain higher [H] within the oxide than that exposed to the reference solution; this may be caused by the expected production of ammonia due to the presence of the nitrate anion as shown in Equation 9.

The practicality and acceptability of adding inhibitors of nitrate containing compounds to the CANDU primary heat transport system is being explored.

## 5 CONCLUSIONS

- 5.1 Depositing a thin Al film on prefilled Zr alloys is found to result in both a reduction in H ingress and increase in corrosion. However, this approach is less practical than adding a chemical compound to the solution. An aluminum acetate compound, however, was not found to have an inhibiting effect when added to high temperature aqueous environments.
- 5.2 Nitrate-containing compounds are found to have an inhibiting effect on H pickup by Zr-2.5 Nb when added to the high temperature aqueous environments, probably as a result of a reduction in available H via the production of ammonia.
- 5.3 The effect of these nitrate-containing compounds on corrosion rate appears to depend on the cation present. This may be the result of these cations being incorporated in the oxide film.



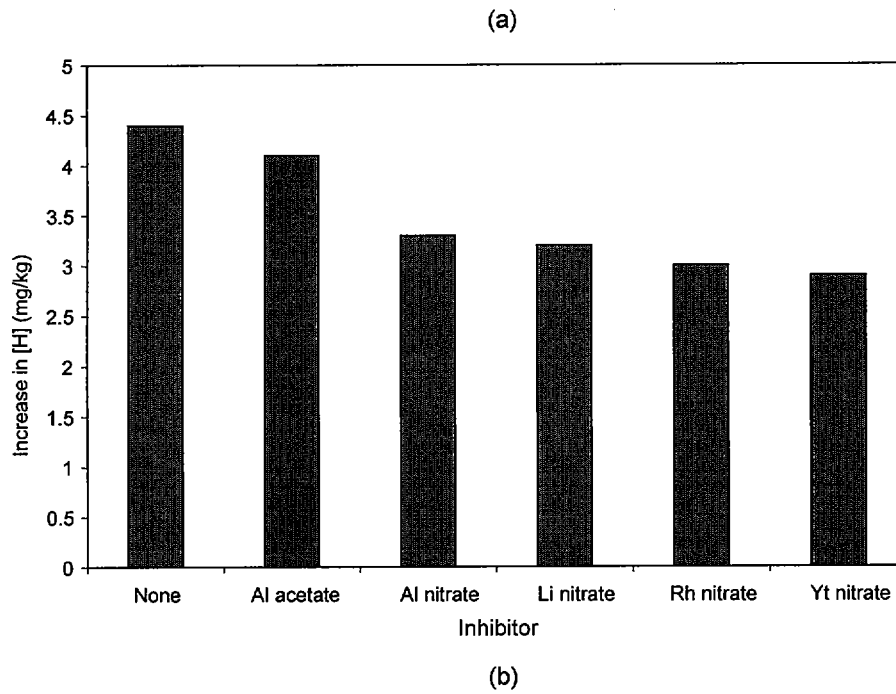


Figure 1 Increase in [H] for various inhibiting additions compared with the reference solution (none) for (a) bare and (b) prefilled samples.

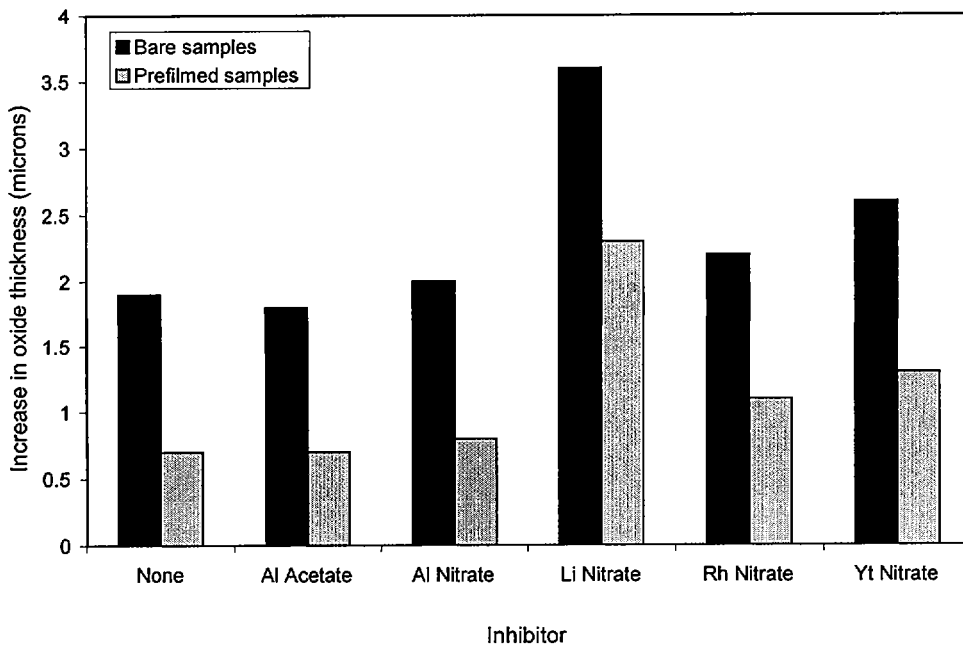
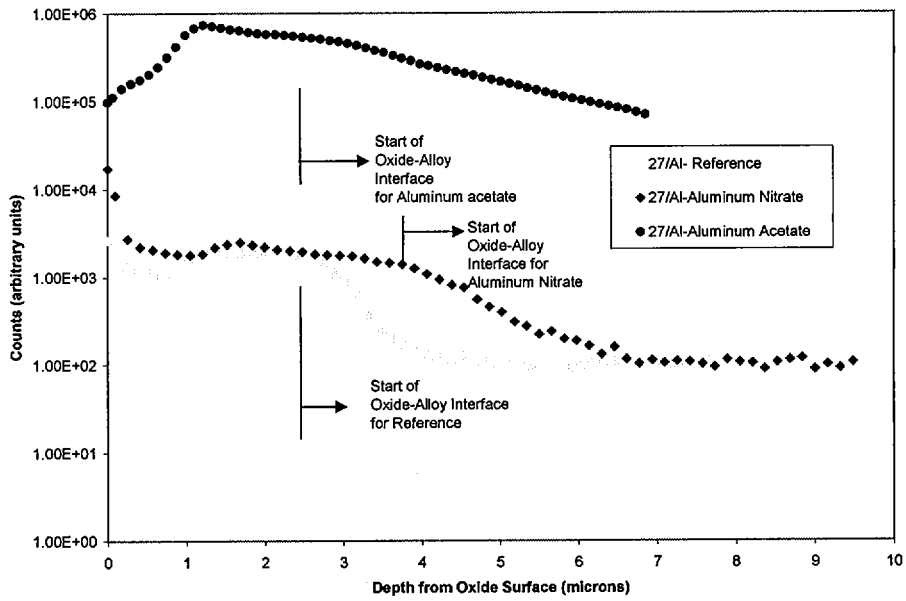
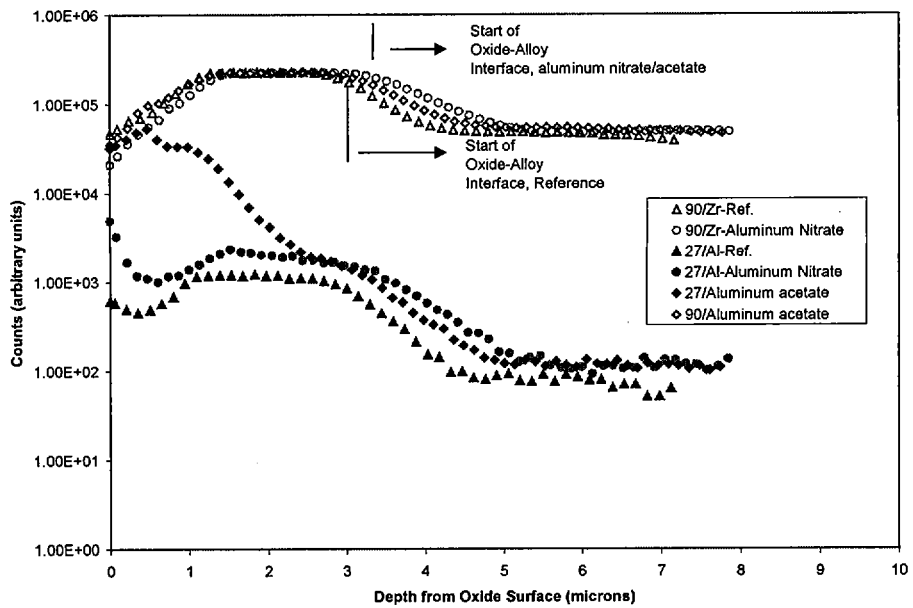


Figure 2 Increase in oxide thickness for both bare and prefilled samples for various inhibiting additions compared with the reference solution (none).



(a)



(b)

Figure 3 Through-oxide-thickness depth profiles using SIMS for oxidized pre-filmed samples showing the incorporation of aluminum into the oxide.

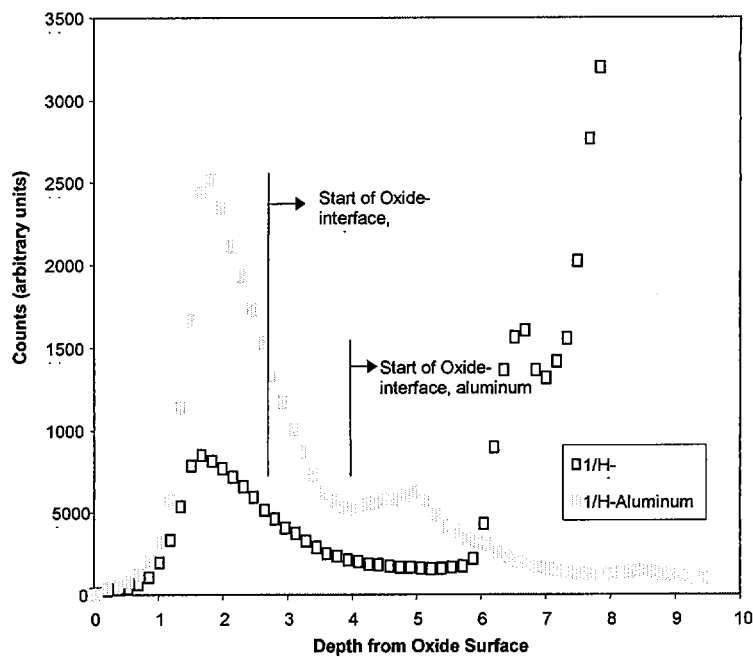


Figure 4 Through-oxide-thickness depth profile by SIMS of mass 1 (H) showing significant reduction in H uptake by the bulk alloy for a bare sample exposed to a nitrate-containing solution compared to the reference solution.

## ACKNOWLEDGEMENTS

The authors acknowledge Mr. Gary Good of Surface Science Western at the University of Western Ontario (Canada) for operating the SIMS instrument.

## REFERENCES

- 1) B. Cox, "Oxidation of Zirconium and its Alloys", *Adv. Corros. Sci. Tech.* 5 173 (1976).
- 2) A.V. Manolescu, E.M. Rasile and P. Mayer, unpublished results (1985).
- 3) J.H. Han, and K.S. Rheem, "The Corrosion Characteristics of Zircaloy-4 Fuel Cladding in LiOH-H<sub>3</sub>BO<sub>3</sub> Solutions", *J. of Nuc. Mat.*, 217 (1994) 197-199.
- 4) H. H. Klepfer, "Hydrogen Uptake of Zirconium Alloys During Water and Steam Corrosion", *Corrosion*, Vol. 19, 1963, pp 285t-291t.
- 5) T. Shober and N. Iniotakis, "Autocatalytic Tritium Adsorption in Niobium and Tantalum at Room Temperature", *J. of the Less-Common Metals*, 172-174 (1991), 1345-1351.
- 6) J. O'M. Bockris and Reddy, "Modern Electrochemistry", V.2.

- 7) H. A. Liebhafsky and E. J. Cairns, "Fuel Cells and Fuel Batteries", John Wiley, New York, 1968.
- 8) P. Marcus and E. Protopoff, "Coadsorption of Sulphur and Hydrogen on Platinum (110) Studied by Radiotracer and Electrochemical Techniques", Surface Science 161 (1985) 533-552.
- 9) G. C. Bond, "Heterogeneous Catalysis: Principles and Applications", Clarendon Press, Oxford (1987).
- 10) G. A. Eloff, C.J. Greyling and P.E. Viljoen, "Improvement in Oxidation Resistance of Zircaloy-4 by Surface Alloying with a Thin Layer of Palladium", J. of Nuc. Mat. 202 (1993) 239-244.
- 11) G. Vigna, L. Lanzani, G. Domizzi, S.E. Bermudez, J. Ovejero-Garcia and R. Piotrkowski, "Effect of Carbides on the Hydriding and Oxidation Behaviour of a Zr-2.5Nb Alloy", J. of Nuc. Mat. 218(1994) 18-29.
- 12) B.D. Warr, V. Perovic, Y.P. Lin and A.C. Wallace, "Role of microchemistry and Microstructure on variability in Corrosion and Deuterium Uptake of Zr-2.5Nb Pressure tube Material", ASTM Proceedings of the Thirteenth International Symposium on Zirconium in the Nuclear Industry, Annecy, France, June 10-14, 2001.
- 13) N.J.M. Wilkins, "Infrared Interference Measurements on Oxide Films on Zirconium", Corros. Sci. 4, 1964, 17-24.
- 14) M. Yoshimura and S. Somiya, "Fine Zirconia Powders by Hydrothermal Processing", Report of the Research Laboratory of Engineering materials, Tokyo Institute of Technology, No.9 (1984) 53-64.